Batteries & Supercaps

Research Article
doi.org/10.1002/batt.202200561

Chemistry Europe
European Chemical Societies Publishing

www.batteries-supercaps.org

Special Collection

Bipolar Isoindoline Nitroxide for Nonaqueous Symmetrical Redox Flow Battery

Benjamin I. Loomans,[a] Steven E. Bottle,[a] and James P. Blinco*[a]

Crossover in non-aqueous redox flow batteries remains a critical challenge to the cycle stability of these devices. The use of bipolar redox-active organic materials (ROM) is an emerging strategy for mitigating crossover. Herein we report the first example of a bipolar ROM derived from an isoindoline nitroxide, a ring class which gives a number of advantages over the more commonly employed piperidines, including greater stability and a 200 mV higher oxidation potential. Through facile synthetic transformation, the unsubstituted isoindoline nitroxide was nitrated to give a novel bipolar molecule, 5-nitro-1,1,3,3-tetramethylisoindoline-2-yloxyl (NTMIO). This material was investigated electrochemically, revealing a reversible oxidation and quasi-reversible reduction giving a cell potential of 2.07 V. NTMIO was then assessed as an active material in both a static and flow battery model, where cycling was observed for both oxidative and reductive redox couples for over 70 and 20 cycles respectively.

Introduction

Renewable energy sources such as wind and solar are critical to creating a sustainable future, with grid-scale energy storage being the key to widespread integration of these inherently intermittent technologies.[1] Redox flow batteries (RFBs) are attractive storage candidates in comparison to other technologies such as pumped hydro and competing electrochemical technologies including NaS or Li-ion due to improved safety, decoupling of power and capacity, and indefinite storage life at full discharge.[2] To date, the most extensively investigated redox flow chemistry has been the all-vanadium redox flow battery (VRFB), first developed by Skyllas-Kazacos.[3–5]

One of the key advantages of the VRFB is that it utilizes vanadium's four oxidation states, with the V(II)/V(III) couple employed as the negolyte and the V(IV)/V(V) couple as the posolyte. If deleterious mixing of the two electrolytes occurs, the redox-active species interconvert with no permanent decay of the battery's capacity.[5] However, the cell voltage of the vanadium RFB is relatively low (1.26 V) and is already encroaching on the accessible redox potential window of water. In fact, this is a significant limitation for all aqueous chemistries, when compared to non-aqueous solvents.[6] Additionally, the fluctuating price of vanadium and the corrosivity and toxicity of the employed electrolytes further limit its appeal.

Redox-active organic molecules (ROMs) by contrast are composed of earth-abundant atoms like carbon and oxygen and can theoretically be fully renewable when synthesized from biomass feedstocks. Furthermore, important properties such as solubility and oxidation potential can be tailored through molecular design.[7] Despite advances in aqueous RFBs, both organic and inorganic, the aforementioned voltage issue of aqueous systems remains. With judicious choice of electrode and electrolyte this window can be extended beyond the thermodynamic limit of 1.23 V for water, but even this is modest.[8] Many organic solvents have a much wider potential window than water: Propylene carbonate (a common solvent in Li-ion batteries) has a window of approximately 6.6 V, and acetonitrile (a commonly used solvent in nonaqueous RFBs) also has a window of over 6 V.[9]

Currently, most reported RFBs are asymmetrical, with distinct redox-active entities acting as the positive and negative couples.[10] This configuration results in increased synthetic complexity and the need for expensive ion exchange membranes employed as separators.[11] Within asymmetric RFBs, electrolyte crossover produces a gradual but irreversible decline in capacity over time because material that diffuses from one electrode compartment to the other is no longer able to participate in charge or discharge reactions. Taking inspiration from the VRFB, symmetric redox flow batteries employ a redox active material that can be both reduced and oxidized, allowing it to be used as both posolyte and negolyte. Consequently, this means that while crossover may still occur with time, the posolyte material will still function as the negolyte and vice versa, resulting in no net loss in capacity.

Piperidine (TEMPO)-based posolytes have been extensively explored in the literature,[12–17] as the reversible nitroxide/N-oxoammonium redox couple of nitroxides is relatively robust.[18] Though not commonly employed in storage devices, nitroxides are also capable of a third oxidation state: a reduction to an

[a] B. I. Loomans, Prof. S. E. Bottle, A/Prof. J. P. Blinco
Centre for Materials Science
School of Chemistry and Physics
Queensland University of Technology (QUT)
2 George Street, Brisbane, QLD 4000, Australia
E-mail: j.blinco@qut.edu.au

Supporting information for this article is available on the WWW under https://doi.org/10.1002/batt.202200561

Special Collection An invited contribution to a Special Collection on Organic Batteries.

Research Article
doi.org/10.1002/batt.202200561
Chemistry Europe
European Chemical Societies Publishing

aminoxyl anion. However, this anion quickly reacts with solvent in a proton transfer reaction, irreversibly producing the neutral hydroxylamine species.[19] Recently, Wylie et al. have showed that this nitroxide/aminoxyl anion redox couple can in fact be stabilized in certain ionic liquids,[20] and this may influence future research directions. Nitronyl nitroxides too are an exception, as the reduced form is persistent due to resonance stabilisation. Duan et al.[21] and Hagemann et al.[22] have utilised this property to produce bipolar battery materials with cell voltages of 1.73 and 1.62 V respectively. However, the former lost 50% capacity over 35 cycles and the latter experienced poor active material utilization due to high viscosity of the electrolyte.

To our knowledge, only one other example exists of an all-organic bipolar molecule created by the combination of a nitroxide with a reversibly reducible moiety. By combining TEMPO and phenazine via a triethylene glycol linker, Winsberg et. al created a molecule with a redox potential of 1.2 V in an aqueous electrolyte.[14] Connecting the two active redox couples through a heteroatomic linkage is relatively atom inefficient and due to the more labile nature of such linkages compared to a fused carbon framework could lead to separation of the two active species.

Herein, we demonstrate a new approach to designing symmetric nitroxide ROMs utilizing the isoindoline carbon framework. Isoindoline based nitroxides, such as 1,1,3,3-tetramethylisoindolin-2-yloxyl (TMIO), have seen use in organic polymer batteries where they compare favorably to commercially available nitroxide polymers such as PTMA.[23–24] Small molecule isoindoline nitroxides have been observed to have oxidation potentials over 200 mV higher than their piperidine counterparts, and the fused aromatic backbone also makes them less prone to ring-opening degradation.[18] Many redox-active negolyte molecules described in literature are aromatic, with nitrobenzene (NB) being among the simplest.[25,26] With the isoindoline aromatic ring being reported to readily undergo nitration in high yield,[28] it was proposed that the resultant molecule, 5-nitro-1,1,3,3-tetramethylisoindolin-2-yloxyl (NTMIO), could act as an atom efficient, carbon fused hybrid of a nitrobenzene negolyte and a nitroxide posolyte (as illustrated in Figure 1). To this end, the molecule was characterized electrochemically and its performance as a posolyte and negolyte were investigated in a both a static and flow liquid battery model.

Results and Discussion

NTMIO was synthesized via an established synthetic route and isolated as an orange crystalline material.[27,28] The nitration reaction carried out directly on the unprotected nitroxide is efficient, high yielding and scalable which is illustrative of the facile transformations capable on the isoindoline core utilising aromatic substitution. To assess the redox activity of NTMIO, it was initially compared to nitrobenzene (NB) and unsubstituted isoindoline (TMIO) via cyclic voltammetry to ensure that hybridization does not drastically alter the electrochemistry of the two moieties. The electrochemical results of these voltammograms are summarized in Table 1.

As can be seen in Table 1, NTMIO undergoes a reversible oxidation comparable to that of the unsubstituted isoindoline nitroxide TMIO (peak anodic/cathodic current ratio 1.04). Furthermore, the oxidation of NTMIO was found to occur 100 mV higher than that of the unsubstituted TMIO. This can be attributed to the strong electron-withdrawing effect of the nitro functional group, thus making the nitroxide moiety harder to oxidise. The reduction of NTMIO occurs at a potential comparable with that of nitrobenzene, although slightly more positive (~ 40 mV). The peak anodic/cathodic current ratio of NTMIO however indicates a quasi-reversible process. Overall, the incorporation of the nitro functionality is advantageous as it

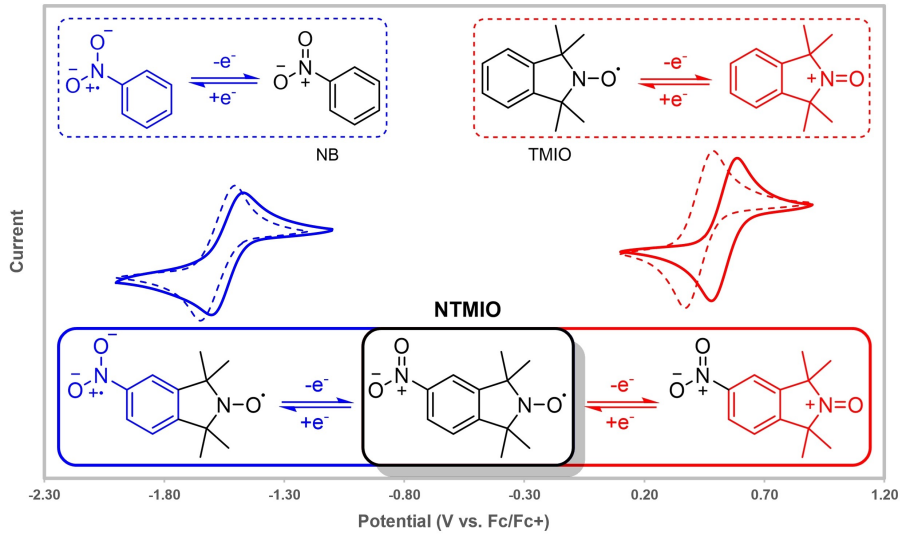

Figure 1. Cyclic voltammograms demonstrating the ability of 5-nitro-1,1,3,3-tetramethylisoindoline-2-yloxyl (NTMIO) to act as both a posolyte (solid red) and negolyte (solid blue). An open circuit voltage of 2.07 V is observed. This is comparable to the voltage that could be achieved in an asymmetric system of nitrobenzene (NB, dashed blue) and isoindoline nitroxide (TMIO, dashed red).

Research Article
doi.org/10.1002/batt.202200561
Chemistry Europe
European Chemical Societies Publishing

Table 1. Summary of redox properties from Figure 1. Potentials are referenced to the ferrocene/ferrocenium redox couple.

Compound	E_{pa} [V]	E_{pc} [V]	$E_{1/2}$ [V]	E_{pc}–E_{pa} [V]	i_{pa}/i_{pc}
NB	−1.648	−1.506	−1.577	0.142	0.96
TMIO	0.370	0.485	0.428	0.115	1.04
NTMIO (red.)	−1.603	−1.479	−1.541	0.124	1.28
NTMIO (ox.)	0.480	0.586	0.533	0.106	1.04

results in a higher overall cell voltage compared to an asymmetric cell composed of the parent molecules.

When exposed to highly reducing applied potentials, further electrochemical processes can be observed for all three molecules, as illustrated in Figure 2. For NTMIO, the first additional reduction process appears to be very poorly reversible, occurring at approximately −2.2 V vs. Fc/Fc^+. The second process is completely irreversible, occurring below −2.5 V. By comparison with the behaviour of its parent materials under these conditions, we identified the likely processes responsible for these additional reductions. The first reduction resembles that of the parent isoindoline, shifted to lower potentials due to the additional electron density supplied by the negative charge of the reduced nitro group. This reduction corresponds to the reduction of the nitroxide to the unstable hydroxylamine anion. The second reduction appears to be analogous to that of nitrobenzene, a further completely irreversible process.

Solubility is a critical factor for a potential RFB material as it is directly proportional to the capacity and energy density of the device. To assess this, a supersaturated solution was prepared in acetonitrile, the supernatant taken and diluted 10,000× and compared to a calibration curve as shown in the supporting information Figure S1.

The solubility of this material was found to be 0.42 M, giving a maximum theoretical capacity of 11 Ah/L and an energy density of 23 Wh/L. This result places NTMIO as having one of the highest theoretical energy densities among reported bipolar redox-active materials.[21,22,29]

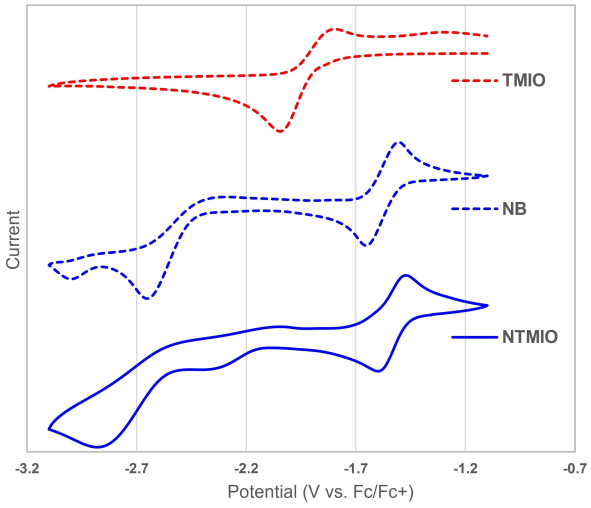

Figure 2. At highly negative applied potentials, the nitroxide moiety of TMIO reduces to a hydroxylamine anion with poor reversibility. Nitrobenzene (NB) also undergoes a further reduction, albeit completely irreversible. NTMIO appears to undergo both processes.

The diffusion coefficient is also an important property for ROMs as diffusion of reactant to the electrode is often the limiting factor in current density and therefore charge rate. Linear sweep voltammetry at a rotating disk electrode (RDE) was used to ascertain the diffusion limited current at various rotation rates (Figure S2a). A Levich plot was constructed (Figure S2b) from this data, the slope of which was used to calculate the diffusion coefficient via the Levich equation. The diffusion coefficient of NTMIO was determined to be 9.5×10^{-6} $cm^2 s^{-1}$, which compares favorably to similar bipolar molecules such as PTIO[20] (6.2×10^{-6} $cm^2 s^{-1}$, and even to prominent asymmetric ROMs N-methylphthalimide and DBMMB[30] (8.38 and 5.77×10^{-6} $cm^2 s^{-1}$, respectively).

To assess the performance and stability of NTMIO as a posolyte and negolyte independently, a static H-cell battery was constructed in a symmetric configuration, with the same electrolyte on both sides of the fritted separator. The electrolyte was composed of a 0.01 M NTMIO solution in acetonitrile with tetrabutylammonium hexafluorophosphate (NBu_4PF_6) as a supporting salt. Due to the high resistance of this kind of cell, the potential of the working electrode was recorded relative to a reference electrode positioned as close as possible within the working electrode chamber.

Initial attempts focused on accessing a 100% state of charge (SOC), operating within a window of +/−450 mV. This window was experimentally determined to allow for full charge and discharge of the materials while accounting for the voltage drop due to internal resistance of the static cell. Under these conditions, the static cell suffered substantial capacity fade within 50 cycles for both oxidative and reductive cycling. The instability of the oxidative cycling (Figure S3) was especially surprising as nitroxides have been previously demonstrated to be robust posolytes under similar conditions.[12] However, the most drastic loss of capacity was produced during reductive cycling (Figure 3 top). While the capacity achieved initially approached 80% of the theoretical value, it decreased rapidly until only ~10% of the theoretical capacity remaining after 70 charge/discharge cycles.

It was hypothesised that the largely irreversible further reductions of NTMIO shown in Figure 2 were also taking place within the static cell, due to the overpotentials required to reach a high state of charge, and that these processes were responsible for the loss of capacity. Other instances of ROMs containing nitro groups as negolyte materials[25,31] have also reported capacity fade due to over-reduction of the nitro group, ultimately culminating in aniline and azobenzene products. To test this hypothesis, two more reductive cycling experiments

Research Article
doi.org/10.1002/batt.202200561
Chemistry Europe
European Chemical Societies Publishing

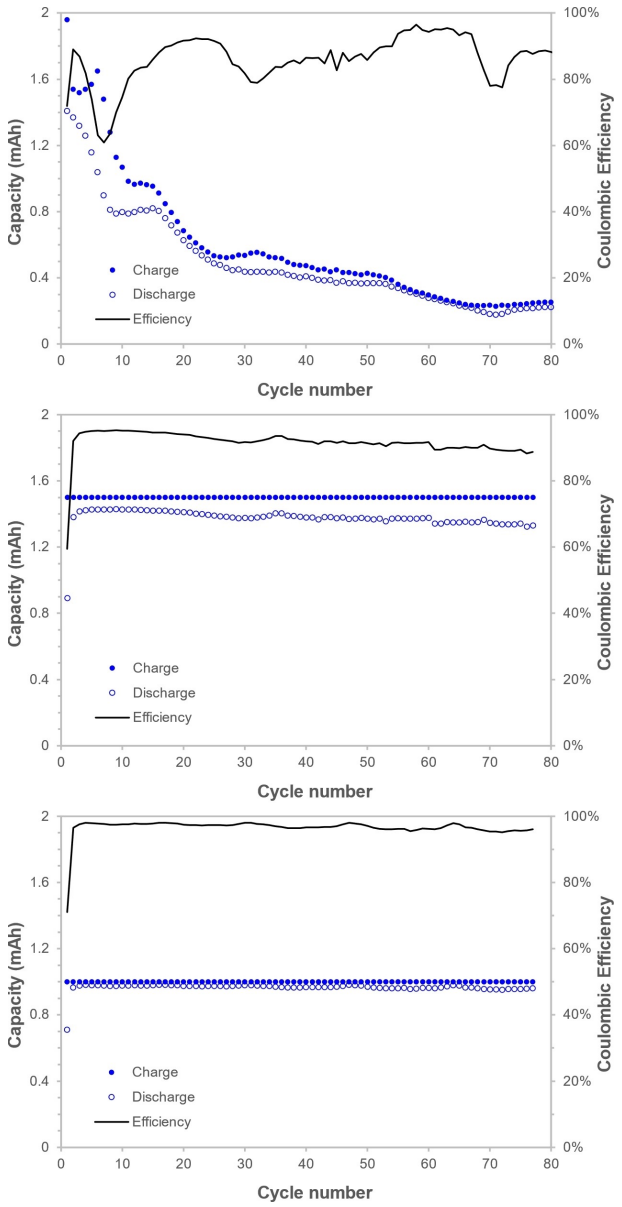

Figure 3. Reductive static cycling of 10 mM NTMIO in 0.1 M tetrabutylammonium hexafluorophosphate (NBu_4PF_6) within a H-Cell. Total volume is 8 mL per chamber, giving a theoretical capacity of 2 mAh. Capacity vs. cycle indicates stability of NTMIO when cycled to 100% (top), 75% (middle) and 50% (bottom) state of charge (SOC). Applying a lower SOC reduced the overpotential the material was exposed to and thus the opportunity for over-reduction of NTMIO. This yielded more stable continual cycling and better columbic efficiency of the cell.

were subsequently conducted in the static cell at lower states of charge, thus limiting the overpotential applied to the active material.

This milder approach yielded a substantial improvement in the reductive cycle stability, as can be seen in the contrast between the capacity retention of the 100% SOC experiment (Figure 3 top) and the 75 and 50% SOC experiments (Figure 3 middle and bottom, respectively). In addition to limiting the galvanostatic charging time for the latter two experiments, potentiostatic holds were also implemented on discharge to minimize a slow increase of SOC due to incomplete discharge compounding over several cycles.

Despite maintaining capacity for its duration, the 75% SOC experiment underwent a gradual decrease in coulombic efficiency. It is possible that even at 75% SOC, small quantities of NTMIO are lost to over-reduction in each cycle. As the excess material was consumed by this process, the actual SOC slowly increased, thereby exacerbating this decomposition pathway and consuming more material per cycle. This could account for the gradual decrease in coulombic efficiency as the experiment continued. However, it should be noted that not all of the coulombic losses can be due to decomposition as if this were the case the on average 10% losses per cycle would have quickly added up to 100%. Instead, some of the coulombic inefficiency is likely due to crossover of the charged material.

Reducing the applied SOC to 50% greatly improved coulombic efficiency (>97% vs. ~90%), further supporting the hypothesized link between applied potential and degradation of the material. Interestingly, when examining the potential profile over time of this experiment (Figures S12 and S13), a new plateau gradually appears at a potential 200 mV higher than the main NTMIO reduction. Some of the products of nitrobenzene reduction are themselves electroactive and reversible, and azobenzenes have even been employed in nonaqueous RFBs.[32] It is plausible that this new plateau is due to products of NTMIO over-reduction as observed by other groups.

To further confirm the reduction of NTMIO as the source of cycle instability, oxidative cycling was also conducted at 75% SOC. Like the reductive cycling, the cell was charging to 75% of its theoretical capacity, then discharged with a potentiostatic hold. Interestingly, despite a much better coulombic efficiency throughout the experiment than for the analogous reductive experiment (Figure 3 middle vs. Figure 4), the battery started to lose capacity after 30 cycles. After 80 cycles, the capacity had dropped to 1.17 mAh, or just under 60% of the theoretical capacity. This result was again unexpected, because as discussed earlier, nitroxides have previously been demonstrated to be

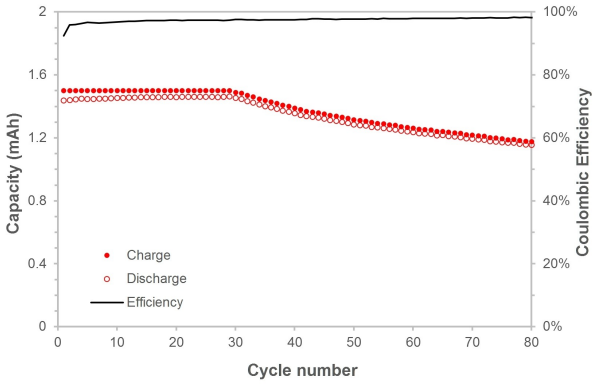

Figure 4. Oxidative static cycling of NTMIO (0.01 M) to 75% state of charge. While columbic efficiency remains high, a gradual capacity fade is observed from cycle 30. This may be attributed to degradation of NTMIO in the counter electrode chamber producing a concentration gradient, leading to loss of active material from the working electrode chamber by diffusion through the frit.

Research Article
doi.org/10.1002/batt.202200561
Chemistry Europe
European Chemical Societies Publishing

highly robust posolyte materials. However, the much higher retained coulombic efficiency of this experiment supports the concept that the loss of capacity likely originated from the counter electrode rather than from the working side. As the counter electrode in a static cell is subjected to an unregulated overpotential

(whereby it functions to balance the charge from the working electrode), it is plausible that irreversible over-reduction of NTMIO occurred at the counter electrode during this experiment. Material is then lost from the working side via gradual diffusion through the separator due to the concentration gradient formed by the destruction of material in the counter electrode chamber.

Taking into account the sensitivity of the active material to over reduction, both the 100% (Figure 5 top) and 50% (Figure 5 bottom) state of charge flow cell tests were undertaken. As with the static cell experiments, the 100% SOC underwent rapid capacity fade where less than 20% of the original capacity was obtained after 20 cycles. Under the same conditions, but limiting at 50% SOC there was little to no loss of capacity over the same number of cycles. However soon after cycle 20, the cell underwent a rapid and catastrophic failure. We believe that this could be due, again, to issues with over reduction. In a static cell, overpotentials due to changing cell resistance because of separator or electrode ageing is corrected for by the reference electrode. Within a flow cell however, these processes cannot be corrected for and as a result, over-reduction of NTMIO can easily occur.

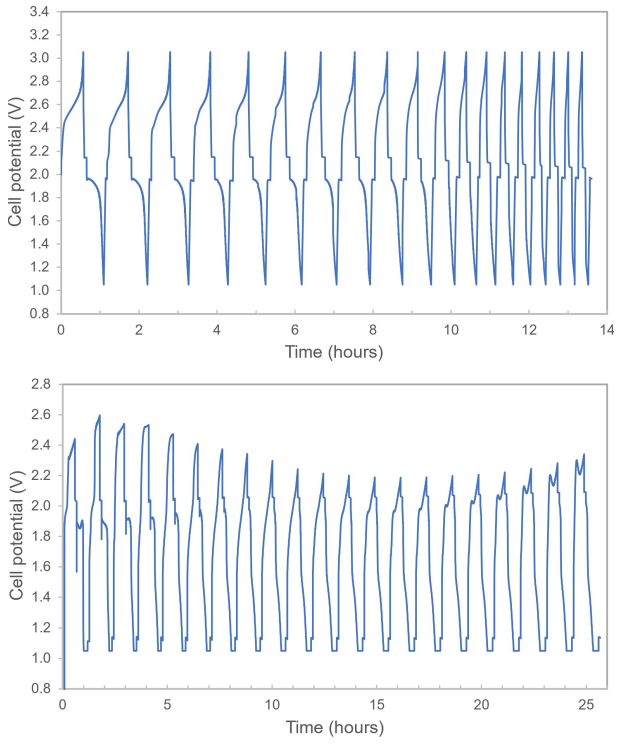

Figure 5. Flow cell cycling of NTMIO (0.05 M) to 100% SOC (top) and 50% SOC (bottom). Charging was conducted at a rate of 1 C, or 13.4 mA. Akin to static cell experiments, a rapid loss of capacity occurred in the 100% SOC experiment over 20 cycles whereas capacity was maintained for the 50% SOC.

Conclusion

A bipolar molecule containing the first example of an isoindoline nitroxide ROM has been successfully demonstrated. It was characterised electrochemically, showing a synergistic effect between the nitro and nitroxide moieties leading to a cell voltage of 2.07 V. Further, its suitability as an energy storage molecule was demonstrated in a static H-cell. When stressing the system by cycling to 100% SOC, significant capacity fade was observed, likely due to the irreversible over-reduction of NTMIO. The effect of this over-reduction could be mitigated through milder charge/discharge cycling. Moving to lower SOC cycling, the issues of over-reduction could be mitigated, and the static cell could be subjected to over 70 charge/discharge cycles while maintaining good coulombic efficiencies over 90% with no observed loss of capacity. Flow cell cycling further reinforced the need for a more robust reductive group to pair with the isoindoline nitroxide moiety. In future, investigation of isoindoline-based BRMs using other reductive moieties should eliminate the need for this mild approach. The highlighted advantages of using the isoindoline backbone as a fused carbon scaffold to produce bipolar redox active materials should facilitate this in future efforts toward novel green electroactive battery materials.

Experimental Section

General: All electrochemistry experiments were controlled by a BioLogic SP-150 potentiostat and EC-Lab software. The reference electrode employed was either a leakless Ag/AgCl electrode (ET069-1, eDAQ) (−0.35 V vs. Fc/Fc+), or an Ag/Ag^+ single-junction non-aqueous electrode (echem-ref-r-sr, Ionode, QLD, Australia) composed of 0.01 M $AgNO_3$ and 0.1 M tetrabutylammonium hexafluorophosphate (NBu_4PF_6) in acetonitrile contacting a silver wire (−0.10 V vs. Fc/Fc+). NTMIO was synthesised in 4 steps from *N*-benzylphthalimide in an overall yield of 30% according to literature procedures.[27,28]

Cyclic voltammetry: All CV experiments were performed in a glovebox under nitrogen atmosphere. The working electrode was a 3 mm diameter glassy carbon electrode, a length of platinum wire served as the counter electrode, and the non-aqueous Ag/Ag+ electrode was employed as a reference. The active materials were diluted to 0.01 M in dry acetonitrile with NBu_4PF_6 0.1 M as supporting salt. Each experiment was performed at a scan rate of 100 mV/s.

Rotating disk electrode: Experiments using the rotating disk electrode were performed with a 5 mm diameter glassy carbon working electrode, a length of platinum wire as a counter electrode, and the leakless Ag/AgCl electrode as a reference. The active solution was composed of 0.1 M NBu_4PF_6 as supporting salt and 0.01 M NTMIO in acetonitrile, which was then sparged with argon for 10 minutes prior to taking measurements. A stream of argon was maintained over the solution's surface during the experiment.

H-Cell cycling: Charge/discharge experiments were performed in a custom H-cell composed of a 2 mm thick, porosity 5 glass frit separator, reticulated vitreous carbon (RVC) foam (ERG Aerospace)

working and counter electrodes, and the leakless Ag/AgCl electrode as a reference. The electrolyte solution was prepared under a nitrogen atmosphere within a glovebox and was composed of 0.01 M NTMIO active material and 0.1 M NBu_4PF_6 dissolved in acetonitrile dried over 4a molecular sieves. 8 mL of the electrolyte was added to the working and counter electrode chambers. The electrodes were then added, and the cell left to equilibrate overnight. Each half-cell was magnetically stirred at 400 rpm with a 5 mm Teflon coated stir bar. Galvanostatic charging was performed at 2 mA (1 C charging rate).

Flow cell cycling: A flow cell was constructed following a device reported in the literature.[33] Kalrez® (FKKM) o-rings were used for their high resistance to solvents and chemically harsh environments. Gaskets were cut from 0.5 mm expanded PTFE sheeting (Gore GR, W. L. Gore & Associates). The electrodes were composed of 3 pieces of carbon paper (17 mm × 15 mm) for a surface area of 2.55 cm^2 with a nominal thickness of 0.54 mm. A Masterflex™ L/S™ Digital Miniflex Dual-Channel Pump with Norprene peristaltic pump tubing (Saint-Gobain) was used to pump the electrolyte.

The electrolyte was composed of 0.05 M NTMIO in dry MeCN with 0.5 M NBu_4PF_6 as a supporting salt. 10 mL of this solution was added to the reservoirs of the flow cell and pumped at a rate of 10 mL/min. Theoretical capacity of the battery was 13.4 mAh Charge and discharge was performed galvanostatically at a rate of 1 C (13.4 mA, 5.25 mA/cm^2, with a 3 V upper limit and 1 V lower limit.

UV-Vis: UV-vis absorbance spectra used to determine the solubility of NTMIO were recorded on a Shimadzu UV-1800 UV-vis spectrophotometer.

Acknowledgements

We gratefully acknowledge support from Queensland University of Technology, Central Analytical Research Facility (QUT), the Centre for Materials Science (QUT). BIL acknowledges the Centre for Materials Science for a M. Phil research scholarship. JPB acknowledges additional funding from the Future Batteries Industry CRC. Open Access publishing facilitated by Queensland University of Technology, as part of the Wiley - Queensland University of Technology agreement via the Council of Australian University Librarians.

Conflict of Interests

The authors declare no conflict of interest.

Data Availability Statement

The data that support the findings of this study are available in the supplementary material of this article.

Keywords: bipolar redox-active material · high-voltage · nitroxide · non-aqueous flow battery · radical

[1] S. Weitemeyer, D. Kleinhans, T. Vogt, C. Agert, *Renewable Energy* **2015**, *75*, 14–20.
[2] B. Dunn, H. Kamath, J. M. Tarascon, *Science* **2011**, *334*, 928–935.
[3] M. Skyllas-Kazacos, M. A. Green, M. Rychcik, R. G. Robins, A. G. Fane, *J. Electrochem. Soc.* **1986**, *133*, 1057–1058.
[4] M. Skyllas-Kazacos, F. Grossmith, *J. Electrochem. Soc.* **1987**, *134*, 2950–2953.
[5] M. Rychcik, M. Skyllas-Kazacos, *J. Power Sources* **1988**, *22*, 59–67.
[6] R. M. Darling, K. G. Gallagher, J. A. Kowalski, S. Ha, F. R. Brushett, *Energy Environ. Sci.* **2014**, *7*, 3459–3477.
[7] J. Winsberg, T. Hagemann, T. Janoschka, M. D. Hager, U. S. Schubert, *Angew. Chem. Int. Ed.* **2017**, *56*, 686.
[8] J. Zheng, G. Tan, P. Shan, T. Liu, J. Hu, Y. Feng, L. Yang, M. Zhang, Z. Chen, Y. Lin, J. Lu, J. C. Neuefeind, Y. Ren, K. Amine, L.-W. Wang, K. Xu, F. Pan, *Chem* **2018**, *4*, 2872–2882.
[9] K. Gong, Q. Fang, S. Gu, S. F. Y. Li, Y. Yan, *Energy Environ. Sci.* **2015**, *8*, 3515–3530.
[10] Z. Rhodes, J. R. Cabrera-Pardo, M. Li, S. D. Minteer, *Isr. J. Chem.* **2021**, *61*, 101–112.
[11] J. Yuan, Z.-Z. Pan, Y. Jin, Q. Qiu, C. Zhang, Y. Zhao, Y. Li, *J. Power Sources* **2021**, *500*, 229983.
[12] X. Wei, W. Xu, M. Vijayakumar, L. Cosimbescu, T. Liu, V. Sprenkle, W. Wang, *Adv. Mater.* **2014**, *26*, 7649–7653.
[13] T. Janoschka, S. Morgenstern, H. Hiller, C. Friebe, K. Wolkersdörfer, B. Häupler, M. D. Hager, U. S. Schubert, *Polym. Chem.* **2015**, *6*, 7801–7811.
[14] J. Winsberg, C. Stolze, S. Muench, F. Liedl, M. D. Hager, U. S. Schubert, *ACS Energy Lett.* **2016**, *1*, 976–980.
[15] J. Winsberg, T. Janoschka, S. Morgenstern, T. Hagemann, S. Muench, G. Hauffman, J. F. Gohy, M. D. Hager, U. S. Schubert, *Adv. Mater.* **2016**, *28*, 2238–2243.
[16] W. Zhou, W. Liu, M. Qin, Z. Chen, J. Xu, J. Cao, J. Li, *RSC Adv.* **2020**, *10*, 21839–21844.
[17] B. Liu, C. W. Tang, H. Jiang, G. Jia, T. Zhao, *ACS Sustainable Chem. Eng.* **2021**, *9*, 6258–6265.
[18] J. P. Blinco, J. L. Hodgson, B. J. Morrow, J. R. Walker, G. D. Will, M. L. Coote, S. E. Bottle, *J. Org. Chem.* **2008**, *73*, 6763–6771.
[19] X. Wei, W. Pan, W. Duan, A. Hollas, Z. Yang, B. Li, Z. Nie, J. Liu, D. Reed, W. Wang, V. Sprenkle, *ACS Energy Lett.* **2017**, *2*, 2187.
[20] L. Wylie, T. Blesch, R. Freeman, K. Hatakeyama-Sato, K. Oyaizu, M. Yoshizawa-Fujita, E. I. Izgorodina, *ACS Sustainable Chem. Eng.* **2020**, *8*, 17988–17996.
[21] W. Duan, R. S. Vemuri, J. D. Milshtein, S. Laramie, R. D. Dmello, J. Huang, L. Zhang, D. Hu, M. Vijayakumar, W. Wang, J. Liu, R. M. Darling, L. Thompson, K. Smith, J. S. Moore, F. R. Brushett, X. Wei, *J. Mater. Chem. A* **2016**, *4*, 5448–5456.
[22] T. Hagemann, J. Winsberg, B. Häupler, T. Janoschka, J. J. Gruber, A. Wild, U. S. Schubert, *NPG Asia Mater.* **2017**, *9*, e340.
[23] K.-A. Hansen, J. P. Blinco, *Polym. Chem.* **2018**, *9*, 1479–1516.
[24] K.-A. Hansen, J. Nerkar, K. Thomas, S. E. Bottle, A. P. O'Mullane, P. C. Talbot, J. P. Blinco, *ACS Appl. Mater. Interfaces* **2018**, *10*, 7982–7988.
[25] B. Liu, C. W. Tang, C. Zhang, G. Jia, T. Zhao, *Chem. Mater.* **2021**, *33*, 978–986.
[26] X. Yu, W. A. Yu, A. Manthiram, *Energy Storage Mater.* **2020**, *29*, 266–272.
[27] P. Griffiths, G. Moad, E. Rizzardo, *Aust. J. Chem.* **1983**, *36*, 397.
[28] R. Bolton, D. G. Gillies, L. H. Sutcliffe, X. Wu, *J. Chem. Soc. Perkin Trans. 2* **1993**, 2049-2052.
[29] J. Moutet, J. M. Veleta, T. L. Gianetti, *ACS Appl. Energ. Mater.* **2021**, *4*, 9–14.
[30] X. Wei, W. Duan, J. Huang, L. Zhang, B. Li, D. Reed, W. Xu, V. Sprenkle, W. Wang, *ACS Energy Lett.* **2016**, *1*, 705–711.
[31] D. Xu, C. Zhang, Y. Zhen, Y. Li, *ACS Appl. Mater. Interfaces* **2021**, *13*, 35579–35584.
[32] L. Zhang, Y. Qian, R. Feng, Y. Ding, X. Zu, C. Zhang, X. Guo, W. Wang, G. Yu, *Nat. Commun.* **2020**, *11*, 3843.
[33] J. Milshtein, Electrochemical Engineering of Low-Cost and High-Power Redox Flow Batteries, MIT, 2017–04-25.

Manuscript received: December 22, 2022
Revised manuscript received: April 13, 2023
Accepted manuscript online: April 17, 2023
Version of record online: April 27, 2023